

publication, we showed that the p66Shc-dependent apoptosis is a multi-step process in which mitochondria play an important role [14]. PKC β , which is activated by oxidative stress, phosphorylates p66Shc on Ser36 residue what triggers its translocation to the mitochondria. The increased ROS production by mitochondria, as a response to p66Shc translocation, seems to increase the probability of mitochondrial permeability transition pore opening. This in turn leads to the release of proapoptotic cofactors into the cytoplasm and the “mitochondrial” route of apoptosis can be executed. This molecular pathway explains how p66Shc links oxidative challenge with apoptosis and its contribution in aging [14,15].

In this manner, we investigated the level of p66Shc and its Ser36-phosphorylated form in tissues of animals of different age. Following free-radicals theory of aging which says that aging is caused by accumulation of oxidative stress-induced damages, we also determined ROS production and the levels of antioxidant enzymes that protect cells against ROS action.

Materials and methods

Ethics

The animal studies were carried out in accordance with the Guidelines for the Care and Use of Laboratory Animals prepared by the Polish Academy of Sciences and with approval from Local Ethics Committee.

Tissues sample preparation

One day and 1, 3, 5, 6, 10, 12, 23-month-old female NMRI mice were maintained in temperature-controlled cages, fed ad libitum, with free access to water. After decapitation, liver, heart, lung, kidneys and samples of brain, skin, muscle and diaphragm were collected. Tissues were homogenized in a 75 mM sucrose, 225 mM mannitol, 0.1% Triton X100, 30 mM Tris (pH 7.4) buffer containing inhibitors of proteases (1 mM PMSF and protein protease inhibitor cocktail) and phosphatases (1 mM Na₃VO₄, 10 mM NaF). After that equal portion of pre-chilled lysis buffer (50 mM Tris, pH 7.5, 150 mM NaCl, 1% Triton, 0.1% SDS, 1% sodium deoxycholate) containing proteases and phosphatases inhibitors was added to each homogenate. Samples were centrifuged at 14,000g for 20 min at 4 °C to remove debris. Protein concentration in tissue lysates was determined using Bradford method. Samples for SDS-PAGE were denaturated in a reducing Laemmli loading buffer at 95 °C for 5 min.

Subcellular fractionation of mouse liver

Livers from sacrificed animals were cooled (4 °C) and washed in homogenization medium (to remove blood and connective tissue), then cut into small pieces. After that fresh homogenization medium was added of 4 ml/g of liver. Livers were gently disrupted by 15 up-and-down strokes in a Potter-Elvehjem motor-driven homogenizer. The homogenate was centrifuged twice at 750g for 5 min to remove cellular debris and nuclei. The collected supernatant was used for:

(A) Isolation of crude mitochondrial fraction, “pure” mitochondrial fraction, lysosomes, endoplasmic reticulum and cytosolic fraction. Post-nuclear supernatant was centrifuged at 10,300g for 10 min to pellet crude mitochondria. The resultant supernatant was centrifuged at 25,000g for 30 min to obtain enriched lysosomal fraction. Post-lysosomal supernatant was centrifuged at 100,000g for 1 h in a Beckman 70 Ti rotor to pellet microsomes. The final supernatant contained cytosolic proteins. The crude mitochondrial pellet

was resuspended in isolation medium (250 mM mannitol, 5 mM Hepes (pH 7.4), and 0.5 mM EGTA) and layered on top of 8 ml of Percoll medium (225 mM mannitol, 25 mM Hepes (pH 7.4), 1 mM EGTA, and 30% Percoll (v/v)) in a 10-ml polycarbonate ultracentrifuge tube and then centrifuged for 30 min at 95,000g. A dense band containing purified mitochondria was recovered from approximately $\frac{3}{4}$ down the tube. The mitochondrial band was removed, diluted with isolation medium, and washed twice by centrifugation at 6300g for 10 min to remove the Percoll, after which the mitochondria were resuspended in isolation medium. MAM fraction was removed from the Percoll gradient as the diffuse white band located above the mitochondria. Isolation medium was added, and the membranes suspension was centrifuged at 6300g for 10 min. The supernatant containing MAM was centrifuged at 100,000g for 1 h in a Beckman 70 Ti rotor, and the resulting MAM pellet resuspended in homogenization buffer.

(B) Isolation of plasma membrane and plasma membrane-associated membranes. Post-nuclear supernatant was centrifuged at 20,000g for 20 min. Pellet containing crude membranes fraction (plasma membrane, mitochondria and PAM fraction) was suspended in 5 mM Bis-Tris, 0.2 mM EDTA, pH 6.0 and subjected to separation on a discontinuous 38%, 43% and 53% sucrose gradient made on the base of the solution: 5 mM Bis-Tris, 0.2 mM EDTA, pH 6.0. A low-density band localized on the top of 38% sucrose (denoted as the PAM fraction), middle-density band characterized as a crude mitochondrial fraction localized at the 38/43% sucrose interface and a high-density band, 43/53% sucrose interface, (denoted as plasma membrane) were collected and diluted threefold with 225 mM mannitol, 75 mM sucrose, 0.1 mM EGTA, 5 mM Tris-HCl, pH 7.4. PAM fraction was sedimented at 100,000g for 45 min. Purified plasma membrane was centrifuged at 10,000g for 10 min to remove contaminating mitochondria and then sedimented at 48,000g for 20 min.

All isolated subcellular fractions (except cytosol) were suspended in 225 mM mannitol, 75 mM sucrose, 0.1 mM EGTA, 5 mM Tris-HCl, pH 7.4, using a loose-fitting Dounce homogenizer. Protein concentration was determined according to Bradford's method using Bio-Rad protein estimation kit.

Cells

MAFs (mouse adult fibroblasts) derived from wild-type 6- and 23-month-old and from p66Shc overexpressing 6-month-old mice were grown in Dulbecco's modified Eagle's medium (DMEM), supplemented with 10% bovine fetal serum (FBS), in 75 cm² Falcon flasks.

Western blotting

Tissue lysates were electrophoretically separated in 8% or 10% SDS-polyacrylamide gel (BioRad) (25–50 μ g of total protein per lane) and transferred onto PVDF membrane (BioRad). Membranes were blocked using 2–4% non-fat milk in TBS buffer with 0.01% Tween-20 (Sigma-Aldrich) for 1 h. Proteins were detected with anti-p66Shc and anti-Ser36-P-p66Shc monoclonal antibodies (1:1000, Abcam), anti-SOD1 rabbit polyclonal antibodies (1:1000, Santa Cruz), anti-SOD2 goat polyclonal antibodies, anti-catalase monoclonal antibodies, anti-glutathione peroxidase and anti-glutathione reductase rabbit antibodies (1:500, Santa Cruz), anti (ACSL-4), acyl-CoA synthetase long-chain family member 4 (1:1000, Santa Cruz), anti actin (1:10,000, Abcam) followed by secondary HRP-conjugated antibodies (1:5000) from Santa Cruz Biotechnology.

Measurement of mitochondrial H₂O₂ production with Amplex-red

The rate of H₂O₂ production in mitochondria isolated from mouse tissues was determined using the fluorogenic indicator Amplex red in the presence of horseradish peroxidase. The final concentrations of horseradish peroxidase and amplex red were 0.1 unit/ml and 5 μM, respectively. Fluorescence was recorded in a microplate reader (Infinite M200, Tecan, Austria) with 530 nm excitation and 590 nm emission wavelengths. In a typical experiment, 0.1 mg/ml of mitochondria were incubated at 30 °C with glutamate (5 mM) and malate (5 mM) as substrates. Measurements were started by addition of horseradish peroxidase.

Measurement of H₂O₂ production in cultured fibroblasts with CM-H₂DCFDA

The rate of H₂O₂ production was measured with the ROS-sensitive fluorescent probe 5- (and 6)-chloromethyl-2',7'-dichlorohydrofluorescein diacetate (CM-H₂DCFDA). The acetate group of CM-H₂DCFDA is hydrolyzed by esterases inside the cell and it is trapped as a non-fluorescent probe (CM-H₂DCF). Then, ROS increases its fluorescence. Cells grown in 12 well plates were treated with 2 μM CM-H₂DCFDA and fluorescence was recorded in a microplate reader (Infinite M200, Tecan, Austria) with 495 nm excitation and 520 nm emission wavelengths.

Measurement of H₂O₂ production in homogenates of mouse tissues with CM-H₂DCFDA

The rate of H₂O₂ production in homogenates of mouse tissues was determined using CM-H₂DCFDA. The acetate group of CM-H₂DCFDA was hydrolyzed by esterases present in organ/tissues homogenates. Fluorescence was recorded in a microplate reader (Infinite M200, Tecan, Austria) with 495 nm excitation and 520 nm emission wavelengths. In a typical experiment, 1 mg of tissue/organ homogenate was resuspended in 1 ml of homogeniza-

tion buffer containing glutamate (5 mM) and malate (5 mM). Measurements were started by addition of 2 μM CM-H₂DCFDA and fluorescence was recorded in a microplate reader (Infinite M200, Tecan, Austria) with 495 nm excitation and 520 nm emission wavelengths.

Measurement of superoxide (O₂⁻) production in cultured fibroblasts with DHE

MAF cells, grown in 12 well plates, were incubated in the presence of 0.5 μM dihydroethidium (DHE) in glucose (5 mM) containing PBS for 20 min at 37 °C. Cells were washed twice with PBS and fluorescence was recorded in a microplate reader (Infinite M200, Tecan, Austria) with 535 nm excitation and 635 nm emission wavelengths.

Detection of protein modification by oxygen free radicals

The level of oxidized proteins in organ/tissue homogenates was estimated with the use of the OxyBlot Protein Oxidation Detection Kit (Chemicon). Twenty-five micrograms of protein was separated on 10% SDS-polyacrylamide gel and standard protocol was proceeded.

Statistical analysis

Data were calculated using Microsoft™ Excel 2005. Differences in band densities, were analyzed for significance by Student's t test.

Results

p66Shc expression in mouse tissues

The available data on the content of p66Shc in different mouse tissues and organs are based mainly on mRNA studies. In agreement with the RT-PCR data of Pelicci and coworkers [1], our Western blot analysis showed that p66Shc is widely expressed in

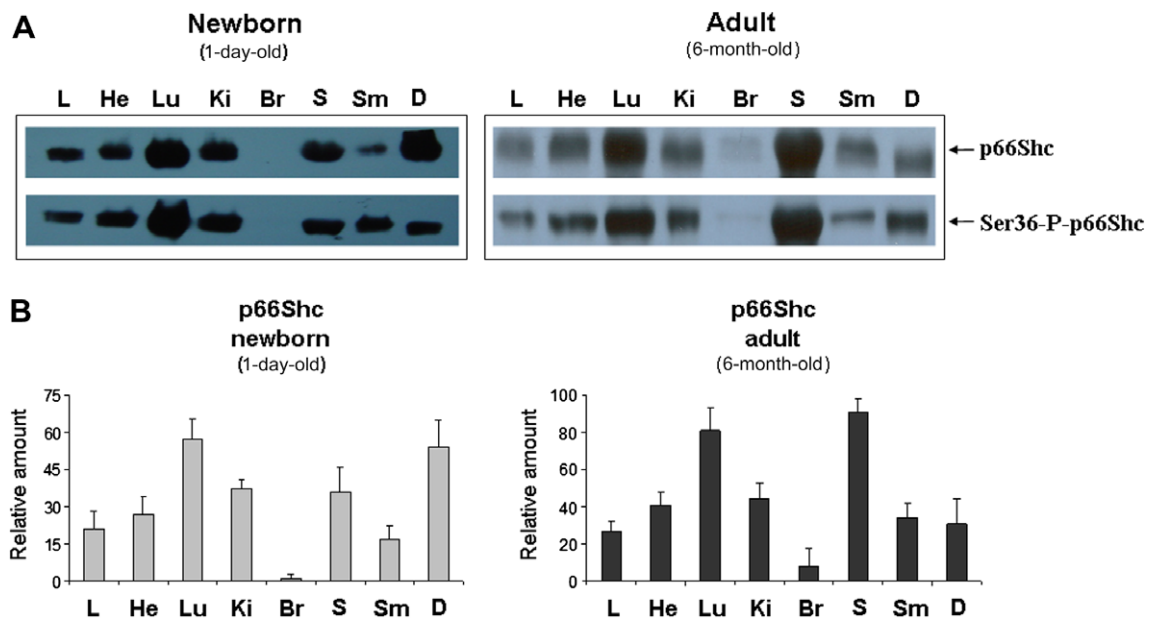


Fig. 1. Expression of p66Shc and its serine 36 phosphorylated form in tissues and organs of newborn (1 day) and 6-month-old mouse. (A) Representative Western blots of p66Shc (top panels) and Ser36-P-p66Shc (bottom panels); Samples (40 μg protein/lane) from 1 day and 6-month-old mouse tissues and organs including liver (L), heart (He), lung (Lu), kidney (Ki), brain (Br), skin (S), skeletal muscle (Sm), diaphragm (D) were separated on 8% (for p66Shc) and 10% gel (for Ser36-P-p66Shc). (B) Densitometric analysis of p66Shc and Ser36-P-p66Shc expression. Coomassie Brilliant Blue G250 staining was performed to calculate relative protein loading. p66Shc and Ser36-P-p66Shc levels were calculated as a ratio to the densitometric values of protein staining. The average of three independent experiments is shown. Each bar represents mean ± SEM (n = 3). Data were analyzed using NIH ImageJ software.

mouse tissues. The highest level of p66Shc protein is observed in lungs and skin, while brain is the only organ with no detectable p66Shc (Fig. 1A and B). Interestingly, the tissue/organ p66Shc and Ser36-P-p66Shc distribution profiles are similar in newborn (1-day-old) and 6-month-old mouse (Fig. 1). The high amount of Ser36-phosphorylated p66Shc in lungs, skin, heart and diaphragm (Fig. 1A) indicates an activation of PKC β pathway and probably enhanced oxidative stress in these organs. The Ser36-P-p66Shc distribution shows similar dependency.

p66Shc and antioxidant enzymes level in tissues and organs of newborn and 6-month-old mice

To look for age-related changes of p66Shc and Ser36-P-p66Shc, we compared their level in organs and tissues from newborn (1-day-old) and in adult 6-month-old mice. The p66Shc and its Ser36-phosphorylated form were significantly elevated in liver, lungs, skin and diaphragm of the older animals (Fig. 2A), that is in tissues regarded as very sensitive to oxidative stress. Although the level of p66Shc did not increase so dramatically in the heart, kidney or skeletal muscle, the level of Ser36-phosphorylated did. The calculated ratio of Ser36-P-p66Shc to the p66Shc is presented in Supplementary Fig. 1. Statistical analysis of data presented in Fig. 2A is presented in Supplementary Fig. 2A.

To check whether the increased level of p66Shc and its Ser36-phosphorylated form in adult 6-month-old mouse modulates the antioxidant defense system, we determined the expression profile of antioxidant enzymes (SOD1, cytosolic superoxide dismutase; SOD2, mitochondrial superoxide dismutase; CAT, catalase; (GR),

glutathione reductase and (GPx), glutathione peroxidase) in tissues/organs from newborn and 6-month-old mice. Results presented in Fig. 2B indicate that the age-dependent phosphorylation of p66Shc at Ser36 is accompanied by modulation of mitochondrial antioxidant defense. This is supported by the observation that although the SOD1 level was fairly constant and the SOD2 and (CAT) were significantly up-regulated in 6-month-old mice. As before, statistical analysis of these data is presented in Supplementary Fig. 2B. In lungs and skin, where a high amount of p66Shc was observed, we detected the lowest age-related increase of the SOD2 level what can be a consequence of the previously described low FKHR-L1 activity in these organs [6].

To verify the hypothesis that there can be a causative link between the level of p66Shc or Ser36-P-p66Shc and the level of antioxidant enzymes we analyzed the effect of p66Shc overexpression (and simultaneously increased level of Ser36-P-p66Shc) in adult mouse fibroblast (MAF's) on enzymes participating in antioxidant defense. As it is presented in Supplementary Fig. 3 both in primary cultures of fibroblasts obtained from 5-month-old mice overexpressing p66Shc and from 18-month-old wild type mouse, higher level of Ser36-P-p66Shc is detected comparing to fibroblast culture from 6-month-old wild type mouse. Moreover, in these cell cultures a significant increase of SOD2 level was observed while SOD1 and CAT levels were unaffected. A substantial increase in the level of SOD2 is probably responsible for decreased superoxide production in these cells (Supplementary Fig. 3B). Interestingly, the rate of H₂O₂ production in all fibroblasts cultures from adult, old wild type mice and in p66Shc overexpressing ones is comparable. This observation can be explained by efficient antioxidant activity

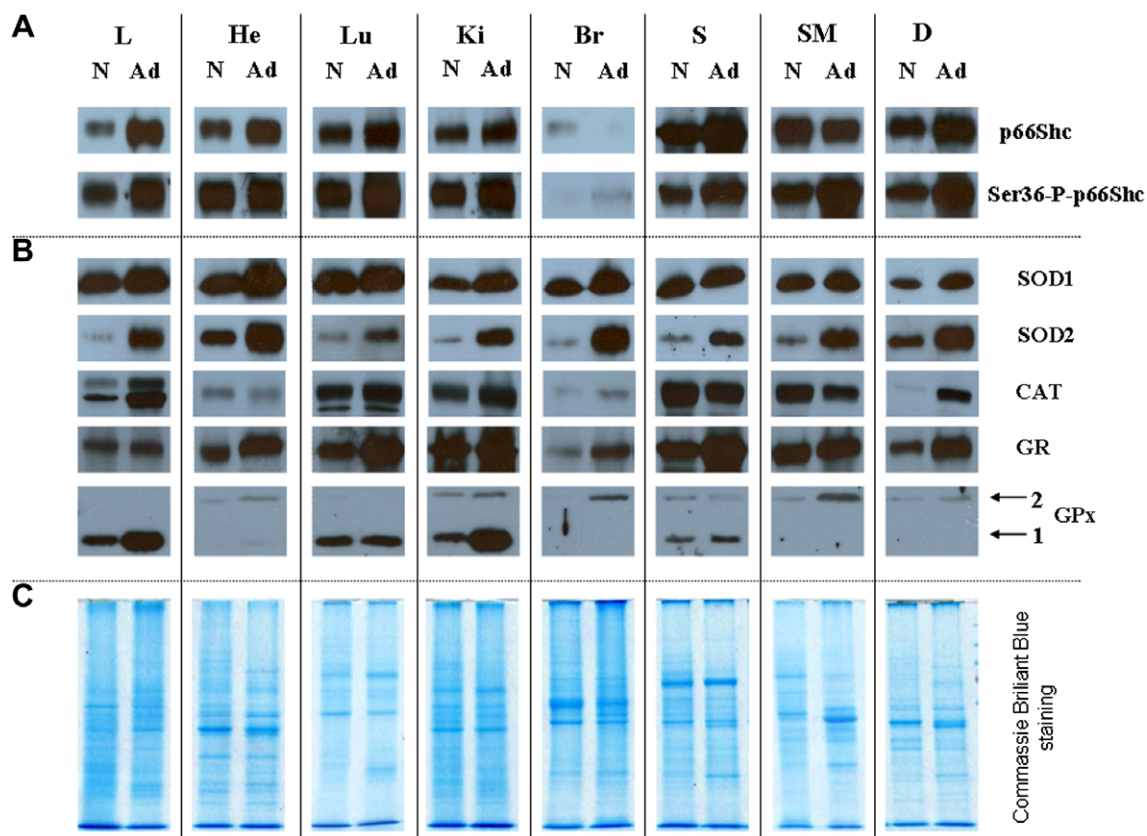


Fig. 2. Age-dependent expression of p66Shc, Ser36-P-p66Shc and antioxidant enzymes in organs and mouse tissues. (A) Age-dependent changes of p66Shc and Ser36-phosphorylated p66Shc; (B) Expression profile of oxidative stress components in different organs and tissues from newborn (N) and 6-month-old (Ad) mouse; SOD1, cytosolic superoxide dismutase; SOD2, mitochondrial superoxide dismutase; CAT, catalase; (GR), glutathione reductase and (GPx), glutathione peroxidase; (C) Coomassie Brilliant Blue G250 staining was used as loading control; A representative immunoblots are shown; Tissue lysates (40 μ g of protein/lane) were separated on 8% or 10% SDS-polyacrylamide gel. Quantification of Western blots is presented in Supplementary Fig. 2.

of CAT. Presented results suggest, that increased level of Ser36-P-p66Shc (not p66Shc – see fibroblasts from 18-month-old mouse) due to enhanced oxidative stress can modulate the level of SOD2, what designates mitochondria as a target of Ser36-P-p66Shc-dependent oxidative stress.

Age-dependent changes of p66Shc, Ser36-P-p66Shc and antioxidant enzymes level in mouse liver

Since significant differences were observed in the levels of p66Shc, SOD2 and Ser36-phosphorylated p66Shc between newborn and adult 6-month-old mice, to better understanding their relevance to the age of animal we performed more detailed time point analysis of the Shc proteins and antioxidant enzymes level in mice livers (see Fig. 3). Apart from significant differences between newborn and older animals, we found that between first and twenty-third month of animal life the level of p46Shc and p52Shc isoforms is relatively constant, but a significant correlation was observed between the age of animals and the level of p66Shc and Ser36-P-p66Shc (Fig. 3). Initially, high level of p66Shc (1, 3, 5 month) decreased and from 6 to 23 month stayed significantly lower. Opposite, low level of Ser36-P-p66Shc (1 day and 1 month) dramatically increased at third month remained constantly high to the twenty-third month of animal life. At the same time the level of CAT and SOD1 did not change significantly between first and tenth month and then considerably decreased. The most visible age-dependent changes in the level of GPX 1, GR and mitochondrial SOD2 have been observed. Moreover, similar relation between age of animal and Ser36-P-p66Shc level was observed also in lung, diaphragm and skin (Supplementary Fig. 4). This can partially explain higher oxidative stress increasing with age, which for liver,

diaphragm, lung and skeletal muscles can be convincingly demonstrated by higher “total” (measured in tissues/organs homogenates) or mitochondrial H_2O_2 production (Supplementary Fig. 5). Increased oxidative stress in old animals was confirmed by the estimation of protein modifications by free radicals in the organs/tissue of 1-month- and 23-month-old mice (see Supplementary Fig. 6).

Intracellular localization of p66Shc

An interesting issue crucial for understanding the role of p66Shc is the intracellular localization of this protein. Although many years have passed since the discovery of p66Shc protein, its mitochondrial localization still represents an open question. To resolve this problem we performed detailed subcellular fractionation of livers homogenates obtained from 1- to 23-month-old mice. Western blotting of isolated fractions presented in Fig. 4 showed that in 23-month-old mice amount of p66Shc localized in crude mitochondria is relatively small comparing with its content in the homogenate and the cytosolic fraction. In crude mitochondria isolated from 1-month-old mouse the level of p66Shc is much lower if not detectable with this amount of protein loaded on the gel. Interestingly, the p66Shc protein was also found in two “special” subcellular fractions: plasma membrane-associated membranes (PAM) and mitochondria-associated membranes (MAM). These fractions can be isolated by purification of crude plasma membrane or crude mitochondria, respectively. Interestingly, calculated ratio of PAM-associated p66Shc level to the MAM-associated one clearly indicates the role that p66Shc can play at the different stage of the organism growth. In 1-month-old mouse there is more p66Shc in PAM fraction (comparing to the MAM), where this

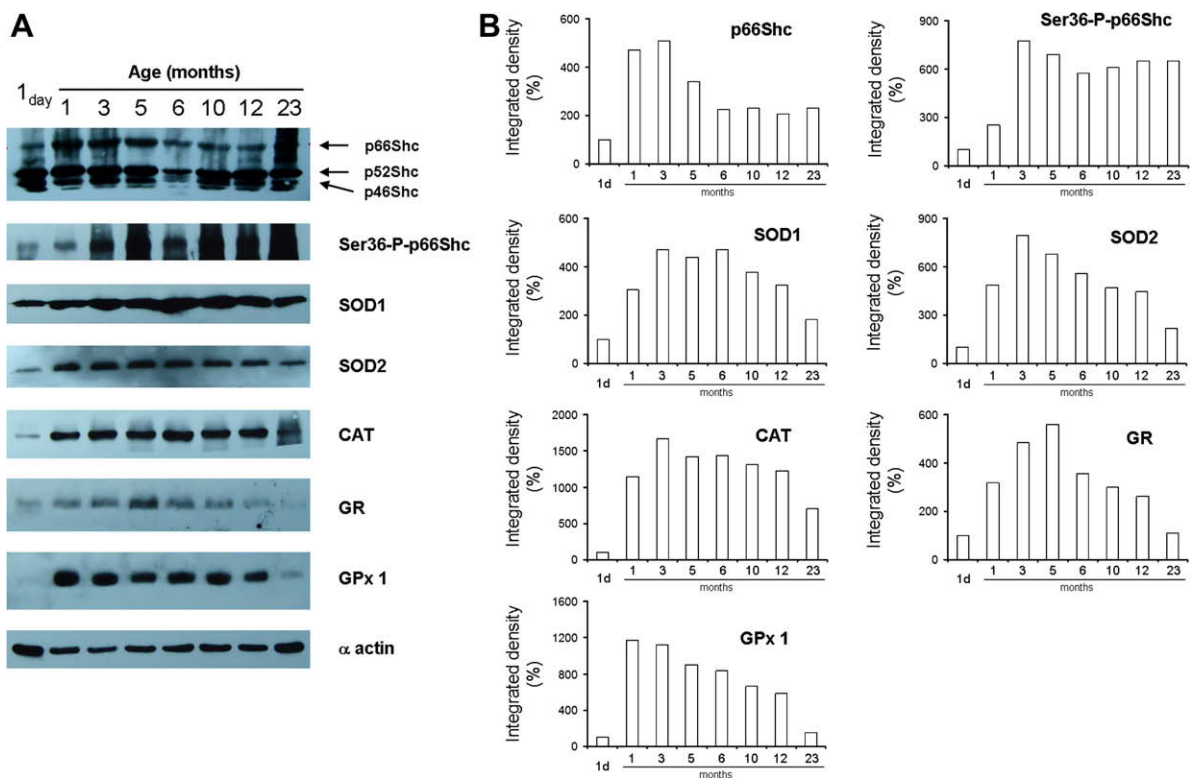


Fig. 3. Age-dependent changes in the level of Shc proteins, Ser36-P-p66Shc and antioxidant enzymes in homogenates from mice livers at different ages (1-day-old, 1, 3, 5, 6, 10, 12, 23-month-old mice); (A) Representative Western blot analysis of Shc proteins, Ser36-P-p66Shc, SOD1; SOD2; CAT; (GR) and (GPX 1). α -actin was used as a loading control. Total lysates (40 μ g protein/lane) were separated on 6% or 10% SDS gel. Result of one immunoblots panel from two independent experiments is shown. (B) Bar chart showing the age-dependent expression of p66Shc, Ser36-P-p66Shc, SOD1, SOD2, CAT, GR and GPX 1. The level of individual proteins were calculated as a ratio to α -actin. Presented values are means from two independent experiments.

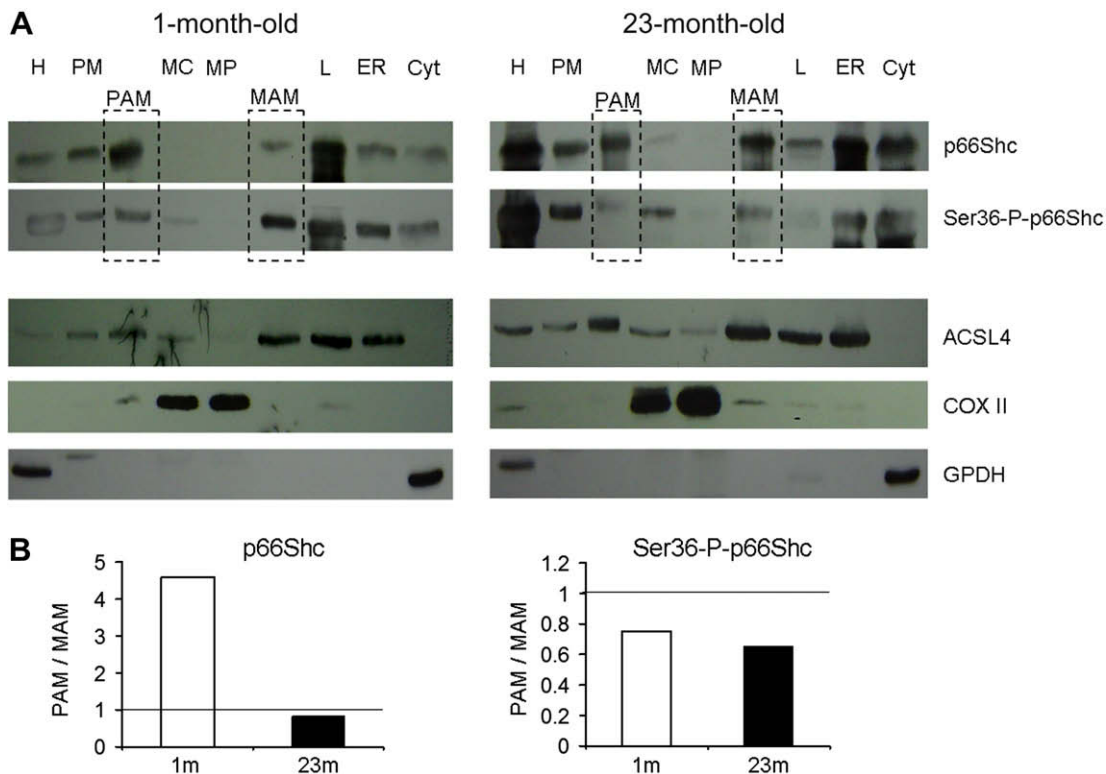


Fig. 4. Age-dependent intracellular localization of p66Shc and Ser36-P-p66Shc. (A) Western blot analysis of subcellular fractions: (H), homogenate; (PM), plasma membrane; (PAM), plasma membrane-associated membranes; (MC), crude mitochondrial fraction; (MP), “pure” mitochondrial fraction; (MAM), mitochondria-associated membranes; (L), lysosomes; (ER), endoplasmic reticulum; (Cyt), cytosol isolated from livers of 1 and 23-month-old mouse. (ACSL-4), acyl-CoA synthetase long-chain family member four was used as a PAM and MAM enrichment marker; COX II was used as a mitochondrial marker, GPDH was used as a cytosolic marker. Subcellular fractions were (40 μ g of protein/lane) were separated on 6% or 10% SDS gel. Result of one immunoblots panel from two independent experiments is shown. (B) Bar charts showing the age-dependent distribution of p66Shc and Ser36-P-p66Shc in MAM and PAM fractions isolated from livers of 1 month (1m) and 23 month-(23m) old mice. The distribution between these both fractions was calculated as a ratio (PAM/MAM) of the level of individual proteins in corresponding fractions. Presented values are means from two independent experiments.

protein is probably involved in the regulation of signal transduction from the epidermal growth factor receptor. In old animal (23-month-old) more p66Shc is present in MAM fraction what can indicate its role in the “induction” of mitochondrial oxidative stress. Moreover, Ser36-P-p66Shc “associated” with crude liver mitochondria was more abundant in 23-month-old mouse, what can partially explain the higher mitochondrial H_2O_2 production observed in older animals (see [Supplementary Figs. 5 and 7](#)). This implicates the MAM as the origin of the mitochondrial p66Shc pool, and partially explains earlier contradictory observations described in the literature.

Discussion

Abnormally elevated ROS production by mitochondria in response to p66Shc phosphorylation increases the probability of cell death. This may be the way in which p66Shc regulates the mitochondrial clock controlling mouse lifespan [15].

In particular, tissue- and age-dependent differences in the amount of p66Shc and its Ser36-phosphorylated form appear to be an interesting issue, because during oxidative stress this Shc protein can be responsible for a formation of pathological signals with different intensity (depending on tissue and age), which can be finally addressed to mitochondria. Expression profile of p66Shc does not depend on mouse age. In both newborn and 6-month-old mice the highest level of p66Shc protein was observed in lungs and skin, while brain was the only organ with no detectable p66Shc. Accordingly to the literature, expression of Shc genes in nervous system is switched during prenatal development from

the A to the C subfamily [16], which explains the lack of p66Shc in the mouse brain. Similarly, the high amount of Ser36-P-Shc was detected in lungs, skin, heart and diaphragm indicating a high activation of PKC β pathway and higher oxidative stress in these organs. A comparison of the p66Shc levels in different tissues/organs from both newborn and adult 6-month-old mice showed a significant increase of this protein in adult animals. This specific age-dependent increase of p66Shc level is probably connected with another role of this protein – its involvement in the signal transduction pathway from the epidermal growth factor receptor to the nucleus. Previous studies indicated that p66Shc is a dominant negative regulator of p46Shc- or p52Shc Ras-mediated signaling pathway, because it competes with p46Shc and p52Shc for Grb2 binding. In this way, p66Shc seems to modulate the strength of signal leading to cell proliferation. This suggests that the low level of p66Shc allows for a higher rate of cells proliferation in tissues and organs of newborn mice. Unfortunately, the role of p66Shc in mouse aging model is in contrast with the Pandolfi’s observation that p66Shc is highly expressed in fibroblasts from centenarians [17]. Our observations indicate that the level of p66Shc in fibroblasts derived from 23-month-old mouse is similar to the observed in fibroblasts from adult 6 month-old.

Despite the increase in the level of p66Shc during the first period of animal development, between the first and fifth month of mouse life the level of p66Shc protein in mouse liver is high and approximately constant but after that decreases and stays significantly lower to twenty-third month. However, the level of the Ser36-P-p66Shc is strictly correlated with age and remains constantly high. This may contribute to the described in the literature

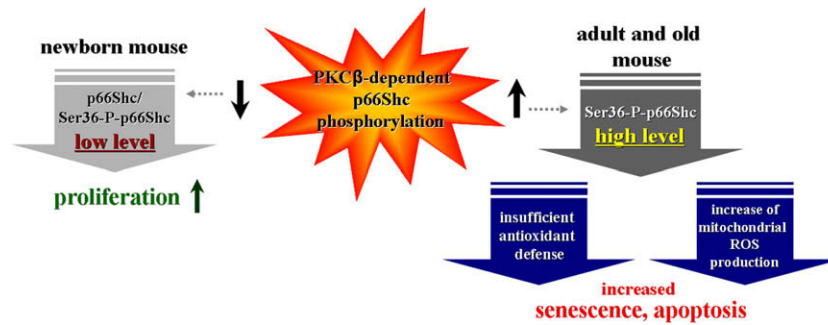


Fig. 5. Hypothetical diagram showing age-dependent correlations between oxidative stress, the level of p66Shc and its Ser36-phosphorylated form and antioxidant defense.

and confirmed also by us the higher superoxide and hydrogen peroxide (H_2O_2) production observed in hepatocytes of old animals [18]. The cell does not stay unprotected during oxidative stress, because of a wide spectrum of antioxidant enzymes that neutralize e.g., superoxide and H_2O_2 [19]. Our studies indicated that an increased level of Ser36-phosphorylated p66Shc accompanies a higher rate of H_2O_2 production in mitochondria isolated from livers of older animals what is in agreement with the observations made by Sohal et al. [20]. In parallel, we observed that the level of CAT and SOD1 did not change significantly between first and tenth month but then considerably decreased. At the same time decreasing levels of GPX 1, GR and mitochondrial SOD2 have been observed. Lower level of mitochondrial SOD2 may suggest the age-correlated decrease of mitochondrial antioxidant defense. The way in which p66Shc may be involved in regulation of antioxidant defense is reviewed in latest paper of Pani et al. [21]. Shortly, the FoxO3a transcription factor which belongs to the family of FoxO proteins is responsible for energy metabolism, proliferation and cell death. Interestingly, FoxO transcription factors regulate the level of SOD2 and catalase because they have the binding site in their promoters and therefore can induce their expression. Since p66Shc act negatively on FoxO, indirectly can decrease amount of antioxidant enzymes like SOD2 and catalase. Our results obtained with the use of fibroblasts cultures derived from old mouse fully support the model proposed by Pani [21], but unexpectedly fibroblasts from p66Shc overexpressing mice also demonstrated the higher level of SOD2. This can be explained only by the (p66Shc independent) cellular response to the oxidative stress resulting in up-regulation of SOD2 level.

An additional issue crucial for understanding of molecular mechanism of p66Shc action is the intracellular localization of this protein. p66Shc has a mitochondrial targeting signal which enables accumulation of p66Shc in this organelle [22]. Indeed, in higher organisms about 20% of fibroblast p66Shc is localized in crude mitochondria fraction and in a response to an oxidative stress part of the cytosolic pool of p66Shc translocates to mitochondria [14,22,23]. The mitochondrial localization of p66Shc is still an open question. It has been proposed that p66Shc localizes within the mitochondrial intermembrane space where it might interact with cytochrome *c* [15] or with glutathione and thioredoxins [24]. By binding to cytochrome *c* p66Shc can act as an oxidoreductase, shuttling electrons from cytochrome *c* to molecular oxygen [15]. Another possible mechanism of signal transduction to the mitochondria by p66Shc also resulting in elevation of ROS production is an interaction of p66Shc with proteins from the outer mitochondrial membrane, e.g., NADH – cyt_b5 reductase, but this possibility requires further studies. Interestingly, in 1-month-old mouse more p66Shc is localized in PAM fraction than in the MAM. This indicates, that at the early stage of animal growth this protein is mostly involved in the regulation of signal transduction from the epidermal growth factor receptor to the nucleus. In old mouse more

p66Shc is present in MAM fraction indicating its translocation to the mitochondria and participation in the mitochondrial oxidative stress (Fig. 5). Also, this can partially explain the higher rate of mitochondrial H_2O_2 production (paralleled by an increased level of Ser36-P-p66Shc) in mitochondria isolated from liver, lung and skeletal muscle of older animals. Interesting studies of Nemoto et al. showed that p66Shc can also regulate mitochondrial metabolism. Overexpression of p66Shc in p66Shc^{-/-} cells increases both oxygen consumption and NADH metabolism [25].

All these data together with our findings support the role free radicals in aging, stating that mitochondria and mitochondria-associated membranes are the main site of age-dependent accumulation of damages caused by free radicals. Three processes contribute to aging progress, the first one – acceleration of the p66Shc-dependent ROS production, second – age-dependent damage of respiratory chain components and the third – an efficiency of mitochondrial antioxidant defense decreasing with age [26].

Acknowledgments

This work was supported by the Polish State Committee for Scientific Research Grant N301 092 32/3407 and Polish Mitochondrial Network.

Appendix A. Supplementary data

Supplementary data associated with this article can be found, in the online version, at doi:10.1016/j.abb.2009.03.007.

References

- [1] G. Pelicci, L. Lanfranccone, F. Grignani, J. McGlade, F. Cavallo, G. Forni, I. Nicoletti, F. Grignani, T. Pawson, P.G. Pelicci, Cell 70 (1992) 90–104.
- [2] S. Okada, A.W. Kao, B.P. Ceresa, P. Blaikie, B. Margolis, J.E. Pessin, J. Biol. Chem. 272 (1997) 28042–28049.
- [3] E. Migliaccio, S. Mele, A.E. Salcini, G. Pelicci, K.M. Lai, G. Superti-Furga, T. Pawson, P.P. Di Fiore, L. Lanfranccone, P.G. Pelicci, EMBO J. 16 (1997) 706–716.
- [4] E. Migliaccio, M. Giorgio, S. Mele, G. Pelicci, P. Reboldi, P.P. Pandolfi, L. Lanfranccone, P.G. Pelicci, Nature 402 (1999) 309–313.
- [5] A. Faisal, M. el-Shemerly, D. Hess, Y. Nagamine, J. Biol. Chem. 277 (2002) 30144–30152.
- [6] S. Nemoto, T. Finkiel, Science 295 (2002) 2450–2452.
- [7] S. Le, T.J. Connors, A.C. Marroney, J. Biol. Chem. 276 (2001) 48332–48336.
- [8] L. Luzi, S. Confalonieri, P.P. Di Fiore, P.G. Pelicci, Curr. Opin. Genet. Dev. 10 (2000) 668–674.
- [9] E.D. Tang, G. Nunez, F.G. Barr, K.L. Guan, J. Biol. Chem. 274 (1999) 16741–16746.
- [10] D. Harman, Mutat. Res. 275 (1992) 257–266.
- [11] R.S. Sohal, Aging Clin. Exp. Res. 5 (1993) 3–17.
- [12] L.J. Yan, R.L. Levine, R.S. Sohal, Proc. Natl. Acad. Sci. USA 94 (1997) 11168–11172.
- [13] G.S. Lopes, O.A. Mora, P. Cerri, F.P. Faria, N.H. Jurkiewicz, A. Jurkiewicz, S.S. Smaili, Biochim. Biophys. Acta 1658 (2004) 187–194.
- [14] P. Pinton, A. Rimessi, S. Marchi, F. Orsini, E. Migliaccio, M. Giorgio, C. Contursi, S. Minucci, F. Mantovani, M.R. Wieckowski, G. Del Sal, P.G. Pelicci, R. Rizzuto, Science 315 (2007) 659–663.

- [15] M. Giorgio, E. Migliaccio, F. Orsini, D. Paolucci, M. Moroni, C. Contursi, G. Pelliccia, L. Luzi, S. Minucci, M. Marcaccio, P. Pinton, R. Rizzuto, P. Bernardi, F. Paolucci, P.G. Pelicci, *Cell* 122 (2005) 221–233.
- [16] L. Conti, C. De Fraja, M. Gulisano, E. Migliaccio, S. Govoni, E. Cattaneo, *Proc. Natl. Acad. Sci. USA* 94 (1997) 8185–8190.
- [17] S. Pandolfi, M. Bonafè, L. Di Tella, L. Tiberi, S. Salvioli, D. Monti, S. Sorbi, C. Franceschi, *Mech. Ageing Dev.* 126 (2005) 839–844.
- [18] T.M. Hagen, D.L. Yowe, J.C. Bartholomew, C.M. Wehr, K.L. Do, J.Y. Park, *Proc. Natl. Acad. Sci. USA* 94 (1997) 3064–3069.
- [19] K.B. Beckman, B.N. Ames, *Oxidants Antioxidants and Aging Oxidative Stress and the Molecular Biology of Antioxidant Defenses*, Cold Spring Harbor Laboratory Press, New York, USA, 1997 (201–246).
- [20] R.S. Sohal, S. Agarwal, B.H. Sohal, *Mech. Ageing Dev.* 81 (1995) 15–25.
- [21] G. Pani, O.R. Koch, T. Galeotti, *Int. J. Biochem. Cell Biol.* 41 (2009) 1002–1005.
- [22] A. Ventura, M. Maccarana, V.A. Raker, P.G. Pelicci, *J. Biol. Chem.* 279 (2004) 2299–2306.
- [23] F. Orsini, E. Migliaccio, M. Moroni, C. Contursi, V.A. Raker, D. Piccini, I. Martin-Padura, G. Pelliccia, M. Trinei, M. Bono, C. Puri, C. Tacchetti, M. Ferrini, R. Mannucci, I. Nicoletti, L. Lanfrancone, M. Giorgio, P.G. Pelicci, *J. Biol. Chem.* 279 (2004) 25689–25695.
- [24] M. Gertz, F. Fischer, D. Wolters, C. Steegborn, *Proc. Natl. Acad. Sci. USA* 105 (2008) 5705–5709.
- [25] S. Nemoto, C.A. Combs, S. French, B.H. Ahn, M.M. Fergusson, R.S. Balaban, T. Finkel, *J. Biol. Chem.* 281 (2006) 10555–10560.
- [26] L. Guarente, C. Kenyon, *Nature* 408 (2000) 255–262.